Theory of acoustic-phonon assisted magnetotransport in two-dimensional electron systems at large filling factors

O. E. Raichev
Institute of Semiconductor Physics, National Academy of Sciences of Ukraine, Prospekt Nauki 41, 03028 Kiev, Ukraine
(Received 11 June 2009; published 25 August 2009)

A microscopic theory of the phonon-induced resistance oscillations in weak perpendicular magnetic fields is presented. The calculations are based on the consideration of interaction of two-dimensional electrons with three-dimensional (bulk) acoustic phonons and take into account anisotropy of the phonon spectrum in cubic crystals. The magnetoresistance is calculated for [001]-grown GaAs quantum wells. The results are in agreement with available experimental data. Apart from the numerical results, analytical expressions for the oscillating part of magnetoresistance are obtained. These expressions are valid in the region of high-order magnetophonon resonances and describe the oscillating magnetoresistance determined by several groups of phonons polarized along certain high-symmetry directions.

DOI: 10.1103/PhysRevB.80.075318 PACS number(s): 73.23.−b, 73.43.Qt, 73.63.Hs

I. INTRODUCTION

In recent years, experimental studies of transport properties of high-mobility two-dimensional (2D) electron gas in weak perpendicular magnetic fields have uncovered a variety of remarkable quantum phenomena caused by transitions of electrons between different Landau levels. Such transitions can lead to oscillations of dissipative resistance as a function of the magnetic field. For example, under steady-state microwave illumination of the 2D gas the resistance oscillates with a period determined by the ratio of the radiation frequency to the cyclotron frequency ω_c. This phenomenon is known as the microwave-induced resistance oscillations (MIRO).[1] For a sufficiently high radiation power the MIRO minima evolve into the intervals of magnetic field where the dissipative resistance vanishes.[2,3] Next, it was found that an increase in the electric current passing though the 2D layer substantially reduces the resistance[4,5] and leads to oscillations of the resistance as a function of either the magnetic field or the current.[4,6,7] Such oscillations are controlled by the ratio of a characteristic energy, which is defined as the drop of the Hall electric field across the classical cyclotron diameter, to the cyclotron energy. This phenomenon has been called the Hall field-induced resistance oscillations (HIRO). It is also described in terms of Zener tunneling between Landau levels. Finally, in the systems with two occupied 2D subbands the resistivity oscillates as a function of the ratio of subband separation energy to the cyclotron energy owing to coupling of the subbands via intersubband scattering. This phenomenon, called the magneto-intersubband oscillations (MISO), is important in the systems with small subband separation, such as the double quantum wells.[8,9] All these kinds of oscillations are insensitive to positions of the Landau levels with respect to the Fermi energy. Therefore, unlike the Shubnikov-de Haas oscillations, they are not damped exponentially with increasing temperature.

The oscillatory phenomena described above require the presence of microwave illumination, strong Hall field, or intersubband coupling to enable resonant transitions between different Landau levels via elastic scattering of electrons by impurities or other static imperfections of the system. The elastic scattering provides the main contribution to resistivity at low temperatures. In high-mobility samples, however, inelastic scattering of electrons by acoustic phonons also contributes to transport, and can exceed the impurity-scattering contribution at the temperatures of several Kelvin. Therefore, acoustic-phonon-assisted transitions of electrons between Landau levels become important. Interestingly enough, these transitions in 2D case possess a resonant property and, for this reason, also lead to oscillations of the resistance. Oscillations of this origin have been discovered recently.[10] An analysis of experimental data has suggested that the resistivity acquires an oscillating contribution whose periodicity is determined by the resonant condition

$$2p_F s = n\hbar\omega_c, \tag{1}$$

where p_F is the Fermi momentum of electrons, s is the constant of the order of sound velocity, and n is an integer.[10] This phenomenon has been called the phonon-induced resistance oscillations (PIRO). Similar oscillations have been observed later in the phonon drag thermal power measurements.[11]

Since the quantity in the left-hand side of Eq. (1) is a characteristic phonon energy, the PIRO can be viewed as magnetophonon oscillations. For the case of electron scattering by optical phonons, the magnetophonon oscillations are known for a long time[12] and have been observed both in bulk and 2D[13] systems. The special feature of PIRO, in contrast to the oscillations owing to scattering by optical phonons, is the dependence of magnetophonon resonance on the electron momentum. By emitting or absorbing acoustic phonons, the electrons jump between the Landau levels, and the maximum probability of such transitions is realized under electron backscattering condition, when the phonon wave number q reaches its maximum value $2p_F/\hbar$ in the 2D plane. Initially,[10] this resonant property of the electron-phonon scattering was explained by involving the interface phonon model. Later, by analyzing phonon-assisted transitions between Landau levels, it was found[11] that the bulk phonon

model gives similar results. It is worth noting that the maximum probability of the backscattering processes ($q=2p_F/\hbar$) is not related to the presence of the magnetic field. It reflects a fundamental property of the kinematics of two-dimensional electron scattering by three-dimensional acoustic modes with frequency $\omega_{\mathbf{q}}=s\sqrt{q_\perp^2+q_z^2}$, where $q_\perp$ and q_z are the in-plane and out-of-plane components of the phonon wave vector. It can be shown that the scattering probability, as a function of the phonon frequency, has a logarithmic singularity at the point of transition from the region $\omega_{\mathbf{q}}<2p_Fs/\hbar$, when pure 2D scattering ($q_z=0$) is possible, to the region $\omega_{\mathbf{q}}>2p_Fs/\hbar$, when emission of three-dimensional phonons (with finite q_z) becomes necessary.

The systematic studies of the PIRO are now under way.[14–17] However, current understanding of this phenomenon is far from complete. The characteristic phonon velocity s entering Eq. (1) varies in different experiments[10,14,15,17] in the range from 2.9 to 5.9 km/s, and the origin of such variations is not clear. The problem of the phase of the oscillations has not been discussed. The dependence of the amplitude of the oscillations on temperature and magnetic field has not been investigated in detail, though general features of the experimental dependence have been successfully related[17] to the behavior of the density of electron states in magnetic field. The main difficulty for interpretation of the experimental magnetoresistance is the complicated nature of acoustic-phonon modes. Even in the case when the influence of interfaces on the phonon spectrum is neglected (bulk phonon approximation), one should take into account three different phonon branches characterized by anisotropic (i.e., dependent on the direction of phonon momentum) velocities.

In this paper, the theory of PIRO is developed within the bulk phonon approximation. Both deformation-potential and piezoelectric mechanisms of electron-phonon interaction are included into consideration. The anisotropy of phonon spectrum is taken into account. The calculations are carried out for GaAs quantum well layers grown in the [001] crystallographic direction. Apart from the numerical results, approximate analytical expressions for the oscillating part of the phonon-induced resistivity are presented. The results are compared with available experimental data for two kinds of GaAs layers with distinctly different densities and mobilities of 2D electrons.

The paper is organized as follows. Section II contains general description of the resistivity of 2D electrons interacting with acoustic phonons in a weak magnetic field. Section III includes both analytical and numerical results for the resistivity, their comparison with experiment, and discussion. The summary and conclusions are given in the last section.

II. GENERAL FORMALISM

Experimental investigations of phonon-induced resistance oscillations are carried out at low temperatures T satisfying the condition of degenerate electron gas, $T\ll\varepsilon_F$, where ε_F is the Fermi energy. Magnetic fields are weak enough to have many Landau levels populated, $\hbar\omega_c\ll\varepsilon_F$, so the electron transport possesses some quasiclassical features (for example, the electron momentum is still a good quantum number). In the same time, the high quality of the samples ensures that the Landau quantization is not suppressed by scattering at such low magnetic fields. This means that the ratio of the cyclotron frequency ω_c to inverse quantum lifetime $1/\tau_q$ is not too small. Next, since in the high-mobility samples the ratio of transport time to quantum lifetime is large, the oscillations are observed in the regime of classically strong magnetic fields, when the cyclotron frequency is much larger than the inverse transport time $1/\tau_{tr}$. The in-plane transport in this case can be viewed as hopping between cyclotron orbit centers, and the dissipative conductivity σ_d is represented in the form

$$\sigma_d=\frac{2e^2}{TL^2}\sum_{\delta\delta'}f(\varepsilon_\delta)[1-f(\varepsilon_{\delta'})]\nu_{\delta\delta'}(X_\delta-X_{\delta'})^2/2, \qquad (2)$$

where δ is the index of a quantum state of electron, X_δ is the coordinate of the cyclotron orbit center in the direction of motion, $f(\varepsilon)$ is the equilibrium Fermi-Dirac distribution function, L^2 is the normalization area, and ν is the total scattering rate, which is represented as a sum of impurity and phonon scattering contributions: $\nu_{\delta\delta'}=\nu_{\delta\delta'}^{im}+\nu_{\delta\delta'}^{ph}$. Assuming interaction of electrons with equilibrium phonons, the latter contribution is written as

$$\nu_{\delta\delta'}^{ph}=\frac{2\pi}{\hbar}\sum_\lambda\int\frac{d\mathbf{q}}{(2\pi)^3}C_{\lambda\mathbf{q}}|\langle\delta|e^{i\mathbf{q}\cdot\mathbf{r}}|\delta'\rangle|^2[(N_{\lambda\mathbf{q}}+1)\delta(\varepsilon_\delta-\varepsilon_{\delta'}-\hbar\omega_{\lambda\mathbf{q}})+N_{\lambda\mathbf{q}}\delta(\varepsilon_\delta-\varepsilon_{\delta'}+\hbar\omega_{\lambda\mathbf{q}})], \qquad (3)$$

where λ, $\mathbf{q}=(q_x,q_y,q_z)$, and $\omega_{\lambda\mathbf{q}}$ are the phonon mode index, wave vector, and frequency, respectively. Next, $N_{\lambda\mathbf{q}}=[\exp(\hbar\omega_{\lambda\mathbf{q}}/T)-1]^{-1}$ is the Planck distribution function. The interaction is described by the function $C_{\lambda\mathbf{q}}$, which includes both deformation-potential and piezoelectric coupling of electrons to crystal vibrations. Considering only acoustic modes in cubic crystals, the general form of this function is written as follows:

$$C_{\lambda\mathbf{q}}=\frac{\hbar}{2\rho\omega_{\lambda\mathbf{q}}}\left[\mathcal{D}^2\sum_{ij}e_{\lambda\mathbf{q}i}e_{\lambda\mathbf{q}j}q_iq_j+\frac{(eh_{14})^2}{q^4}\sum_{ijk,i'j'k'}\kappa_{ijk}\kappa_{i'j'k'}e_{\lambda\mathbf{q}k}e_{\lambda\mathbf{q}k'}q_iq_jq_{i'}q_{j'}\right], \qquad (4)$$

where $\mathcal{D}$ is the deformation potential constant, h_{14} is the piezoelectric coupling constant, and ρ is the material density. The sums are taken over Cartesian coordinate indices, $e_{\lambda \mathbf{q}i}$ are the components of the unit vector of the mode polarization, and the coefficient κ_{ijk} is equal to unity if all the indices i,j,k are different and equal to zero otherwise. The polarization vectors and the corresponding phonon mode frequencies are found from the eigenstate problem

$$\sum_j [K_{ij}(\mathbf{q}) - \delta_{ij}\rho\omega^2]e_{\lambda \mathbf{q}j} = 0. \tag{5}$$

The dynamical matrix for cubic crystals,

$$K_{ij}(\mathbf{q}) = [(c_{11} - c_{44})q_i^2 + c_{44}q^2]\delta_{ij} + (c_{12} + c_{44})q_i q_j(1 - \delta_{ij}), \tag{6}$$

is written in the elastic approximation and expressed through three elastic constants for which the conventional notations are used. Equation (5) has three solutions describing a high-energy mode (LA), which becomes purely longitudinal for high-symmetry directions ([100], [110], and [111]), and two low-energy modes (TA) which become purely transverse for these directions. Very often, theoretical studies of transport properties of electrons in solids with cubic lattice symmetry are based on the continuum approximation for elastic vibrations, when $c_{44}=(c_{11}-c_{12})/2$ and the phonon spectrum is given by three isotropic branches including one longitudinal mode and two degenerate transverse modes. Whereas this approach gives a reasonably good description of phonon-limited mobilities and applies for calculation of many kinetic coefficients, is not sufficient for description of phonon-induced resistance oscillations in magnetic field, because the anisotropy of the acoustic phonon branches is not weak in most semiconductors and becomes essential in evaluation of resonant scattering between Landau levels.

The quantum states δ in Eq. (2) can be treated as exact eigenstates of electrons interacting with randomly distributed impurities in the presence of a magnetic field. It is convenient to rewrite Eq. (2) through the Green's functions of electrons. Using the basis of Landau eigenstates and specifying the growth axis of the quantum-well layer as z (i.e., the [001] crystallographic direction), one obtains the phonon-induced contribution to the conductivity:

$$\sigma_d^{ph} = \frac{e^2 l_B^2}{2\pi\hbar T}\int_0^\infty dq_\perp q_\perp^3 \int_0^\infty \frac{dq_z}{\pi}|\langle 0|e^{iq_z z}|0\rangle|^2 \times \int_0^{2\pi}\frac{d\varphi}{2\pi}\sum_\lambda C_{\lambda \mathbf{q}}(N_{\lambda \mathbf{q}}+1)\sum_{nn'}\Phi_{nn'}(q_\perp^2 l_B^2/2) \times \int d\varepsilon f(\varepsilon)[1 - f(\varepsilon - \hbar\omega_{\lambda \mathbf{q}})]A_\varepsilon(n')A_{\varepsilon-\hbar\omega_{\lambda \mathbf{q}}}(n), \tag{7}$$

where $q_\perp$ and φ are the absolute value and polar angle of the in-plane component of phonon wave vector, n are the Landau level numbers, and l_B is the magnetic length. The function $\Phi_{nn'}(x)=(n!/n'!)x^{n'-n}e^{-x}[L_n^{n'-n}(x)]^2$, where $L_n^m(x)$ are the Laguerre polynomials, describes scattering in the magnetic field. The squared matrix element of a plane-wave factor, $|\langle 0|e^{iq_z z}|0\rangle|^2$, is determined by the confinement potential which defines the ground state of 2D electrons, $|0\rangle$. Applying the model of a deep rectangular quantum well of width d_w, one can rewrite this squared matrix element as $I(q_z d_w/2)$, where $I(x)=(\sin x/x)^2[1-(x/\pi)^2]^{-2}$. Finally, the spectral function $A_\varepsilon(n)$, which is equal to the imaginary part of the single-electron (advanced) Green's function divided by π, characterizes disorder-induced broadening of electron states. In the Born approximation, this broadening is conveniently described in terms of the quantum lifetime of electron, τ_q. In the absence of impurities (the collisionless limit) $A_\varepsilon(n)$ is reduced to the delta function $\delta(\varepsilon-\varepsilon_n)$, where $\varepsilon_n=\hbar\omega_c(n+1/2)$ is the Landau quantization energy.

The dissipative resistivity measured in experiments using Hall bars is related to the conductivity σ_d according to $\rho_d \simeq \sigma_d/\sigma_H^2$, where $\sigma_H=e^2 n_s/m\omega_c$ is the classical Hall conductivity and n_s is the sheet carrier density. The resistivity is represented as a sum of contributions from electron-impurity and electron-phonon scattering:

$$\rho_d = \rho_{im} + \rho_{ph}, \quad \rho_{im} = \frac{m\nu_{im}}{e^2 n_s}, \quad \rho_{ph} = \frac{m\nu_{ph}}{e^2 n_s}, \tag{8}$$

where ν_{im} and ν_{ph} are the partial scattering rates which depend on the magnetic field. Both ρ_{ph} and ν_{ph} are straightforwardly obtained from σ_d^{ph} of Eq. (7). If the magnetic field is zero, ν_{im} and ν_{ph} are reduced to the inverse transport times due to electron-impurity and electron-phonon interactions, respectively, and Eq. (8) describes the classical (Drude) resistivity.

Let us consider the case of weak magnetic fields, when many Landau levels are occupied. Then one can use smallness of the cyclotron energy $\hbar\omega_c$, phonon energy $\hbar\omega_{\lambda \mathbf{q}}$, disorder-broadening energy $\hbar/\tau_q$, and temperature T with respect to the Fermi energy for evaluation of the expression (7). Owing to the sharp form of the spectral functions, the contribution into the n-sums in Eq. (7) comes from a limited number of Landau levels in the vicinity of the Fermi energy, and these sums can be approximately calculated with the following result:

$$\nu_{ph} = \frac{2m}{\hbar^3 T}\int_0^{2\pi}\frac{d\varphi}{2\pi}\int_0^{2\pi}\frac{d\theta}{2\pi}(1-\cos\theta) \times \int_0^\infty \frac{dq_z}{\pi} I\left(\frac{q_z d_w}{2}\right)\sum_\lambda C_{\lambda \mathbf{q}}(N_{\lambda \mathbf{q}}+1) \times \int d\varepsilon f(\varepsilon)[1 - f(\varepsilon - \hbar\omega_{\lambda \mathbf{q}})]D(\varepsilon)D(\varepsilon - \hbar\omega_{\lambda \mathbf{q}}), \tag{9}$$

where $D(\varepsilon)$ is the dimensionless (i.e., normalized to its zero magnetic field value) density of electron states. The integration over the in-plane phonon wave number $q_\perp$ is replaced in Eq. (9) with the integration over the scattering angle θ according to $q_\perp=2(p_F/\hbar)\sin(\theta/2)$. This emphasizes that the phonon-assisted transport at large filling factors is described within the picture of quasielastic scattering of 2D electrons in the vicinity of the Fermi surface. Under the same assump-

tions, the contribution to the resistivity owing to electron-impurity scattering is given by

$$\nu_{im} = \frac{1}{\tau_{tr}^{im}} \int d\varepsilon \left(-\frac{\partial f(\varepsilon)}{\partial \varepsilon} \right) D^2(\varepsilon), \tag{10}$$

where τ_{tr}^{im} is the transport time for electron-impurity scattering. It is defined according to $1/\tau_{tr}^{im} = (m/2\pi\hbar^3) \int_0^{2\pi} d\theta \; w(2p_F \sin\frac{\theta}{2})(1-\cos\theta)$, where w is the Fourier transform of the random impurity-potential correlator. The self-consistent Born approximation leads to the density of states in the form of an expansion in oscillation harmonics weighted with powers of the Dingle factor $d \equiv \exp(-\pi/\omega_c\tau_q)$ (Refs. 18 and 19):

$$D(\varepsilon) = 1 + 2\sum_{k=1}^{\infty} a_k \cos\frac{2\pi k\varepsilon}{\hbar\omega_c},$$

$$a_k = (-1)^k k^{-1} \exp(-\pi k/\omega_c\tau_q) L_{k-1}^1(2\pi k/\omega_c\tau_q). \tag{11}$$

If the magnetic fields is weak, the Dingle factor is small. This corresponds to the case of overlapping Landau levels, when the density of states is given by a single-harmonic expression, $D(\varepsilon) = 1 - 2d\cos(2\pi\varepsilon/\hbar\omega_c)$. In strong enough magnetic fields the electron system is in the regime of separated Landau levels, when $D(\varepsilon)$ is represented by a periodic sequence of semielliptic peaks centered at the Landau quantization energies ε_n.

The expressions (8)–(11), together with Eqs. (4)–(6) defining the phonon spectrum $\omega_{\lambda\mathbf{q}}$ and the function $C_{\lambda\mathbf{q}}$, give a complete description of the phonon-assisted 2D magnetotransport at large filling factors. The next step in evaluation of the resistivity can be done by calculating the integral over the energy ε. In this procedure, it is reasonable to omit the terms containing oscillating functions of energy under the integral. Such terms are responsible for the Shubnikov-de Haas oscillations, and they are exponentially suppressed with increasing temperature. Thus, the approximation used below corresponds to the condition

$$\frac{2\pi^2 T/\hbar\omega_c}{\sinh(2\pi^2 T/\hbar\omega_c)} \ll 1, \tag{12}$$

which means that the temperature should not be too low. As a result,

$$\nu_{ph} = \int_0^{2\pi} \frac{d\varphi}{2\pi} \int_0^{2\pi} \frac{d\theta}{2\pi} (1-\cos\theta) \times \int_0^{\infty} \frac{du_z}{\pi} I\left(\frac{p_F d_w}{\hbar} u_z \right) \sum_{\lambda} \nu_{\lambda\mathbf{q}} F\left(\frac{\hbar\omega_{\lambda\mathbf{q}}}{2T} \right) \times \left[1 + 2\sum_{k=1}^{\infty} a_k^2 \cos\frac{2\pi k\omega_{\lambda\mathbf{q}}}{\omega_c} \right] \equiv \nu_{ph}^{(0)} + 2\sum_{k=1}^{\infty} a_k^2 \nu_{ph}^{(k)}, \tag{13}$$

where $F(x) = [x/\sinh(x)]^2$ and $u_z = \hbar q_z/2p_F$. The quantity

$$\nu_{\lambda\mathbf{q}} = \frac{4mTp_F C_{\lambda\mathbf{q}}}{\hbar^5 \omega_{\lambda\mathbf{q}}} \tag{14}$$

is an anisotropic scattering rate introduced for convenience purpose. The corresponding result for the impurity-assisted magnetotransport has a simpler form, $\nu_{im} = [1 + 2\Sigma_{k=1}^{\infty} a_k^2]/\tau_{tr}^{im}$, which describes a positive magnetoresistance owing to Landau quantization.[18] The Fermi momentum entering Eqs. (13) and (14) is related to electron density according to $p_F = \hbar\sqrt{2\pi n_s}$.

III. RESULTS AND DISCUSSION

The expression (13) is the central part of this paper. The first term of this expression, $\nu_{ph}^{(0)}$, is responsible for phonon-induced contribution to background resistivity, while the second one corresponds to oscillations of the resistivity as a function of the magnetic field. These oscillations (PIRO) are described in Eq. (13) through a sum of oscillatory harmonics of the scattering rate, $\nu_{ph}^{(k)}$. Because of the complicated form of phonon spectrum, the integrals in Eq. (13) cannot be calculated analytically in the general case. However, an analytical consideration is possible for the oscillating part of ν_{ph}, since this part contains rapidly varying functions of $\omega_{\lambda\mathbf{q}}$ under the integral. To carry out the approximate integration, it is convenient to represent expressions for oscillatory harmonics by using the spherical coordinate system according to $\sin(\theta/2) = u\sin\chi$, $u_z = u\cos\chi$, where $u = \hbar q/2p_F$ is the absolute value of phonon wave vector in the dimensionless form and χ is the inclination angle. In these variables, the phonon spectrum is conveniently written as $\omega_{\lambda\mathbf{q}} = s_{\varphi\chi}^{(\lambda)} q$, where $s_{\varphi\chi}^{(\lambda)}$ is the anisotropic sound velocity for the mode λ. The angles φ and χ determine the direction of the phonon wave vector. As a result,

$$\nu_{ph}^{(k)} = \frac{2}{\pi^2} \sum_{\lambda} \int_0^{2\pi} \frac{d\varphi}{2\pi} \int_0^{\pi} d\chi \int_0^{(\sin\chi)^{-1}} du \times \frac{u^3 \sin^2\chi}{\sqrt{1-u^2\sin^2\chi}} I\left(\frac{p_F d_w}{\hbar} u\cos\chi \right) F\left(\frac{p_F s_{\varphi\chi}^{(\lambda)} u}{T} \right) \times [\nu_{\varphi\chi}^{DA(\lambda)} + u^{-2}\nu_{\varphi\chi}^{PA(\lambda)}] \cos\frac{4\pi k p_F s_{\varphi\chi}^{(\lambda)} u}{\hbar\omega_c}, \tag{15}$$

where $\nu_{\lambda\mathbf{q}}$ given by Eq. (14) is written as the expression in the square brackets; the deformation-potential (DA) and piezoelectric (PA) contributions are separated according to Eq. (4). The main contribution to the integral over u comes from the region $u \simeq (\sin\chi)^{-1}$, and the convergence of this integral is determined by the rapidly oscillating cosine function. The other u-dependent functions, I and F, are slowly varying on the scale of convergence because of $p_F d_w/\hbar \sim 1$ and because of condition (12), respectively. After integrating over u, one obtains

$$\nu_{ph}^{(k)} = \frac{1}{\pi^2}\sum_{\lambda}\int_0^{2\pi}\frac{d\varphi}{2\pi}\int_0^{\pi}d\chi \times \sqrt{\frac{\omega_c \sin\chi}{2kp_F s_{\varphi\chi}^{(\lambda)}}} I\left(\frac{p_F d_w}{\hbar}\cot\chi\right) F\left(\frac{p_F s_{\varphi\chi}^{(\lambda)}}{T\sin\chi}\right) \times [\nu_{\varphi\chi}^{DA(\lambda)}/\sin^2\chi + \nu_{\varphi\chi}^{PA(\lambda)}]\cos\left[\frac{4\pi k p_F s_{\varphi\chi}^{(\lambda)}}{\hbar\omega_c \sin\chi} - \frac{\pi}{4}\right]. \quad (16)$$

The remaining double integral over angular variables can be calculated using the method of fastest descent. Indeed, under the integral we have a rapidly oscillating function (the argument of the cosine in Eq. (16) is assumed to be large), and the main contribution comes from certain regions of φ and χ where $\Phi_{\varphi\chi}^{(\lambda)} \equiv s_{\varphi\chi}^{(\lambda)}/\sin\chi$ varies most slowly. Naturally, these regions are in the close vicinity of the extrema points of the function $\Phi_{\varphi\chi}^{(\lambda)}$. The anisotropic sound velocity $s_{\varphi\chi}^{(\lambda)}$ itself has a number of local maxima, minima, and saddle points, whose positions coincide with some high-symmetry directions in the reciprocal (momentum) space. The number of extrema for $\Phi_{\varphi\chi}^{(\lambda)}$ is smaller because of the factor $1/\sin\chi$. For the mode with the highest velocity (this mode becomes purely longitudinal for high-symmetry directions) the anisotropy is not strong, and all the extrema are only at $\chi=\pi/2$ (zero q_z). The slow modes (which become purely transverse for high-symmetry directions) also have extrema at $\chi=\pi/2$. Since the anisotropy of these modes is stronger, they also may have additional groups of extrema at $\chi=\pi/2\pm\xi$, where $\xi<\pi/4$. Nevertheless, the main contribution of slow (low energy) modes to oscillating magnetoresistance is associated with the extremum $\chi=\pi/2$ for a single mode whose velocity at $\chi=\pi/2$ is independent of the polar angle φ. This mode at $\chi=\pi/2$ is purely transverse and polarized perpendicular to the quantum well plane (direction [001]).

In summary, the analysis shows that the modes effectively contributing to the oscillating part of resistivity are: (i) the transverse mode polarized along [001], whose velocity $s_{T0}=\sqrt{c_{44}/\rho}$ is independent of φ and corresponds to a maximum of $\Phi_{\varphi\chi}^{(\lambda)}$ as a function of χ; (ii) the longitudinal mode with velocity $s_{L0}=\sqrt{c_{11}/\rho}$ polarized along [100] or along equivalent directions ([010], $[\bar{1}00]$, and $[0\bar{1}0]$) corresponding to local minima of $\Phi_{\varphi\chi}^{(\lambda)}$; (iii) the longitudinal mode with velocity $s_{L1}=\sqrt{(c_{11}+c_{12}+2c_{44})/2\rho}$ polarized along [110] or along equivalent directions ($[1\bar{1}0]$, $[\bar{1}10]$, and $[\bar{1}\bar{1}0]$) corresponding to saddle points of $\Phi_{\varphi\chi}^{(\lambda)}$. Accordingly, the oscillatory harmonics of the scattering rate are written as sums of three components:

$$\nu_{ph}^{(k)} = \nu_{T0}^{(k)} + \nu_{L0}^{(k)} + \nu_{L1}^{(k)}, \quad (17)$$

where

$$\nu_{T0}^{(k)} = \frac{(eh_{14})^2 mT\omega_c}{8\pi^2\hbar k b_{T0}\rho s_{T0}^3 p_F^2} F\left(\frac{p_F s_{T0}}{T}\right)\sin\frac{4\pi k p_F s_{T0}}{\hbar\omega_c}, \quad (18)$$

$$\nu_{L0}^{(k)} = \frac{\sqrt{2}\mathcal{D}^2 mT\omega_c^{3/2}}{\pi^3\hbar^{5/2}k^{3/2}b_{L0}\rho s_{L0}^{7/2}p_F^{1/2}} F\left(\frac{p_F s_{L0}}{T}\right)\cos\left(\frac{4\pi k p_F s_{L0}}{\hbar\omega_c} + \frac{\pi}{4}\right), \quad (19)$$

$$\nu_{L1}^{(k)} = \frac{\sqrt{2}\mathcal{D}^2 mT\omega_c^{3/2}}{\pi^3\hbar^{5/2}k^{3/2}b_{L1}\rho s_{L1}^{7/2}p_F^{1/2}} F\left(\frac{p_F s_{L1}}{T}\right)\cos\left(\frac{4\pi k p_F s_{L1}}{\hbar\omega_c} - \frac{\pi}{4}\right). \quad (20)$$

The coefficients of order unity standing in the denominators of these expressions are given by

$$b_{T0}^2 = -1 + \frac{(c_{11}+c_{44}+2c_{12})c_A}{c_{44}(c_{11}+c_{12})}, \quad (21)$$

$$b_{L0}^2 = (1+\gamma)\gamma, \quad \gamma = \frac{(c_{11}+c_{12})c_A}{c_{11}(c_{11}-c_{44})}, \quad (22)$$

and

$$b_{L1}^2 = (1+\beta_1)\beta_2,$$

$$\beta_1 = \frac{(3c_{12}+2c_{44}+c_{11})c_A}{(c_{11}+c_{12}+2c_{44})(c_{11}+c_{12})},$$

$$\beta_2 = \frac{(c_{11}+c_{12})c_A}{(c_{11}+c_{12}+2c_{44})(c_{44}+c_{12})}, \quad (23)$$

where $c_A=2c_{44}+c_{12}-c_{11}$ is the positive quantity characterizing the anisotropy of phonon spectrum. The contribution from transverse phonons is associated with piezoelectric potential, while the contribution from longitudinal phonons is due to deformation potential of electron-phonon interaction.

The accuracy of the analytical approach leading to Eqs. (17)–(20) is not expected to be high for lowest-order PIRO peaks. Nevertheless, the applicability of these equations is steadily improved as one moves to lower magnetic fields and the argument of the oscillating function becomes larger. For such low fields, the rate $\nu_{T0}^{(k)}$ tends to overcome the rates $\nu_{L0}^{(k)}$ and $\nu_{L1}^{(k)}$. However, in the samples with higher electron density, where the characteristic phonon wave number $2p_F/\hbar$ is larger, the deformation-potential mechanism is more significant than the piezoelectric one. Therefore, both transverse-phonon and longitudinal-phonon contributions are important and should be taken into account. Notice also that for weak magnetic fields corresponding to the case of overlapping Landau levels one can take only the lowest harmonic $k=1$ in the sum in Eq. (13). This reduces the oscillating part of phonon-induced transport rate ν_{ph} to a simpler form $2d^2\nu_{ph}^{(1)}$.

For completeness, one can also present the result obtained in the isotropic approximation, where there are a longitudinal mode and two degenerate transverse modes with velocities s_l and s_t, respectively:

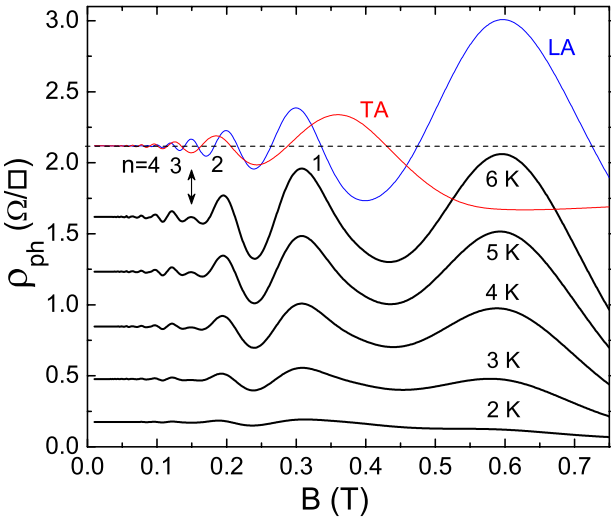

FIG. 1. (Color online) Phonon-induced resistivity calculated for the quantum well of experiment Ref. 17 at temperatures from 2 to 6 K. For $T=6$ K, the partial oscillating contributions from high-energy branch (LA) and low-energy branches (TA) are also shown (shifted for clarity).

$$\nu_{ph}^{(k)} = \frac{(eh_{14})^2 mT\omega_c}{8\pi^2\hbar k\rho s_t^3 p_F^2} F\left(\frac{p_F s_t}{T}\right)\cos\frac{4\pi k p_F s_t}{\hbar\omega_c} + \frac{\mathcal{D}^2 mT\omega_c}{\pi^2\hbar^3 k\rho s_l^3} F\left(\frac{p_F s_l}{T}\right)\cos\frac{4\pi k p_F s_l}{\hbar\omega_c}. \quad (24)$$

In this approximation, the phase of the oscillations, as well as the dependence on magnetic field and Fermi momentum is different from the case of anisotropic phonon spectrum.

The numerical calculations described below use the following elastic constants for GaAs (in units 10^{11} dyn/cm^2): $c_{11}=12.17-0.00144\ T$ (K), $c_{12}=5.46-0.00064\ T$ (K), and $c_{44}=6.16-0.0007\ T$ (K), taken from a semiconductor material database.[20] The temperature dependence of these constants is not really essential in the range of T corresponding to experimental studies of oscillating magnetoresistance. The other GaAs parameters used are $\mathcal{D}=7.17$ eV, $h_{14}=1.2$ V/nm, and $\rho=5.317$ g/cm^3. An example of the results of numerical calculations according to Eq. (13) is presented in Fig. 1. The calculation employs the following parameters of the high-mobility quantum well studied in Ref. 17: $n_s=3.75\times10^{11}$ cm^{-2}, $d_w=30$ nm, impurity-limited mobility 1.17×10^7 cm^2/V s, and quantum lifetime owing to impurity scattering $\tau_q=15$ ps. The theoretical plots are in agreement with experimental data of Ref. 17 as concerns the background resistance, PIRO peak positions, and the amplitude of the oscillations (for example, at $T=4$ K the amplitudes of the peaks numbered 1 and 2 are 0.16 and 0.075 Ohm per square, respectively). The calculation shows that the phonon-induced resistivity is determined by both longitudinal and transverse modes, whose contributions are nearly equal to each other at the fields $B>0.1$ T and at 6 K. At lower fields the transverse-mode contribution becomes more important. With decreasing temperature both contributions are suppressed according to the factor $TF(\hbar\omega_{\lambda\mathbf{q}}/2T)$. The LA-mode contribution is suppressed stronger because the thermal activation energy for this mode is larger. Figure 1 shows that the peak placed slightly below 0.6 T is the lowest-order one for the LA-mode contribution, so the origin of this peak (discussed in Ref. 17) seems to be clear. However, the relative amplitude of this peak is higher than that observed in the experiment, which is possibly related to overestimation of the deformation-potential interaction in comparison to the piezoelectric one.[21] The other low-order peaks ($n=1,2,3$) are formed by both transverse-mode and longitudinal-mode contributions, so their positions B_n are not expected to follow exactly a $1/B$-periodic dependence. Nevertheless, the deviations appear to be small, and a 9-point linear fit of theoretical peak positions (see Fig. 2) gives the dependence $n=2p_F s/\hbar\omega_c-\delta n$, where $s\simeq3.44$ km/s is very close both to the velocity $s_{T0}\simeq3.40$ km/s and to the velocity found experimentally,[17] while $\delta n\simeq0.21$ is slightly larger than that obtained from the experiment.[17] The parameter δn determines the phase of the magnetoresistance oscillations, which appears to be close to the phase of the oscillating factor in the approximate analytical expression (18), $\delta n=1/4$. Starting from $T=3$ K, the theoretical dependence has a weak extra peak (marked by the arrow in Fig. 1) at $B\simeq0.15$ T, which comes from the longitudinal-mode contribution. Though the experimental magnetoresistance[17] does not show a peak in this region, a precursor of such a feature is apparently visible as a flattening of the minimum between the peaks $n=2$ and $n=3$ at the temperatures above 4 K.

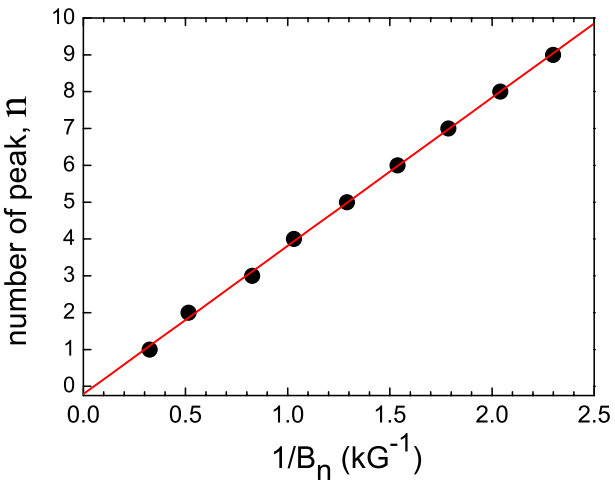

FIG. 2. (Color online) Peak number n as a function of inverse peak position $1/B_n$ extracted from the calculated magnetoresistance (Fig. 1) at 4 K. A linear fit for this dependence yields $s\simeq3.44$ km/s. The same kind of plot based on the experimental data is given in Ref. 17. The positions of low-order peaks slightly deviate from the linear dependence because these peaks are formed by mixture of the oscillating contributions from different phonon modes.

It is important to compare the results of numerical calculation of the oscillating component of phonon-induced magnetoresistance with the results obtained from the analytical approach leading to Eqs. (17)–(20). Figure 3(a) shows the partial contribution of high-energy phonon mode (LA) calculated according to Eq. (13) together with the correspond-

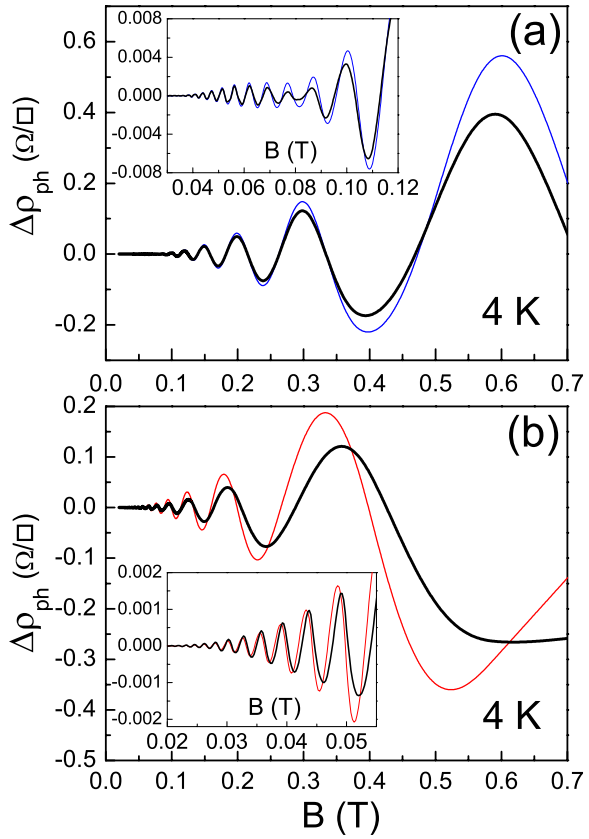

FIG. 3. (Color online) Partial oscillating contributions of the phonon-induced resistivity for the quantum well of experiment Ref. 17 at $T=4$ K. (a) Contribution of high-energy branch (LA). Thick (black) lines correspond to numerical calculation of $\nu_{ph}^{(k)}$ using Eq. (13), and thin (blue) lines are the results obtained from the approximate analytical expressions (19) and (20). The inset shows beating pattern in the low-field region. (b) Contribution of low-energy branches (TA). Thick (black) and thin (red) lines correspond to numerical calculation using Eq. (13) and to approximate analytical expression (18), respectively. The low-field region is shown in the inset.

ing contribution based on the expression $\nu_{ph}^{(k)}=\nu_{L0}^{(k)}+\nu_{L1}^{(k)}$, where $\nu_{L0}^{(k)}$ and $\nu_{L1}^{(k)}$ are given by Eqs. (19) and (20). In a similar way, Fig. 3(b) shows both numerical and analytical, based on Eq. (18), results for low-energy phonon modes (TA). The agreement between exact and approximate results becomes good in the low-field region corresponding to high-order magnetophonon resonances. Both numerical and approximate results in Fig. 3(a) demonstrate a beating pattern with a node at $B\simeq 0.08$ T. The analytical consideration reveals the origin of this beating, since it shows that the oscillations induced by LA phonons are formed as a sum of two contributions, $\nu_{L0}^{(k)}$ and $\nu_{L1}^{(k)}$, with slightly different frequencies.

Figure 4 presents the phonon-induced magnetoresistance calculated for the GaAs quantum wells with $n_s=10^{12}$ cm^{-2} and $d_w=13$ nm studied in Ref. 14. Since the mobility of these samples ($\simeq 6.6\times 10^5$ cm^2/V s at $T=4.2$ K according to the resistance at $B=0$) is much lower than that in Ref. 17, both experimental[14] and theoretical magnetoresistance show a few low-order oscillations. Because of large density and,

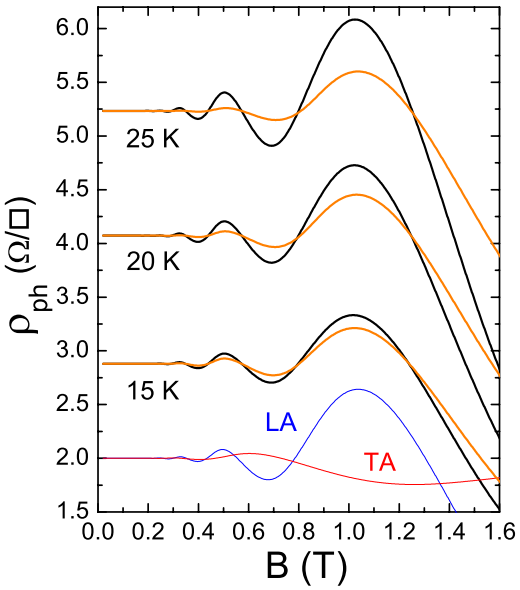

FIG. 4. (Color online) Phonon-induced resistivity calculated for the quantum well of experiment Ref. 14 at different temperatures. For $T=15$ K, the partial oscillating contributions from high-energy branch (LA) and low-energy branches (TA) are also shown (shifted for clarity). The additional (orange) plots take into account temperature-induced decrease of the quantum lifetime and are in a better agreement with experimental data of Ref. 14.

consequently, large Fermi momentum in these samples, the main contribution to oscillating resistivity is caused by the deformation-potential interaction and comes from LA phonons. This is demonstrated by plotting partial contributions of different modes in Fig. 4. At the temperatures 15–25 K all acoustic-phonon modes are fully activated, which means that the function $F(\hbar\omega_{\lambda\mathbf{q}}/2T)$ is close to 1, so the resistivity should linearly increase with temperature. Experimental plots of Ref. 14 indeed show a linear increase for the background resistivity, while the amplitudes of the oscillation peaks depend on T in a different way: the first peak is weakly modified by T and the second peak is suppressed with increasing T. Such a behavior can be explained by a decrease in the quantum lifetime with increasing temperature owing to inelastic electron-electron scattering (see Ref. 17 and references therein). In the present formalism, this effect is described by adding the electron-electron scattering rate $1/\tau_q^{ee}=\lambda T^2/\hbar\varepsilon_F$, where $\lambda\sim 1$, to the inverse quantum lifetime[22] $1/\tau_q$ entering the density of states in Eq. (11). The result of the calculations improved in this way is also shown in Fig. 4. A reasonably good agreement with experimental data, as concerns the amplitudes of the oscillations and their temperature dependence, is achieved at $\lambda=2$.

The positions of the calculated magnetoresistance peaks deviate from the experimental data, though this deviation is not strong. The fitting procedure similar to that shown in Fig. 2 gives the characteristic velocity $s=5.1$ km/s, which is smaller than $s=5.9$ km/s determined in Ref. 14. It is worth noting, however, that the positions of the peaks in the experiment Ref. 14 are shifted to higher magnetic fields as the temperature increases. Though the reason of this shift is not clear, it signifies an increase in experimental velocity s with

temperature. Therefore, one may expect a better agreement of theory and experiment at lower temperatures.

IV. SUMMARY AND CONCLUSIONS

This paper presents a microscopic theory of magnetophonon oscillations, also known as PIRO, in 2D electron systems. The phonon-induced resistivity ρ_{ph} is found by considering both deformation-potential and piezoelectric mechanisms of interaction of 2D electrons with bulk acoustic phonon modes. In the experimentally relevant situation of weak magnetic fields (large filling factors), the expression for the resistivity (or, equivalently, for the phonon-assisted transport rate ν_{ph}) is determined by the electron-phonon coupling constants, phonon frequencies, and the density of electron states in magnetic field; see Eq. (13). The essential feature of the calculations is that the anisotropy of the phonon spectrum is explicitly taken into account. The theory is applied to quantum wells based on the materials of cubic symmetry and grown in the [001] crystallographic direction. For this case, an analytical expression for the oscillating part of the resistivity has been derived. This expression is valid in the region of fields corresponding to high-order magnetophonon resonances, when the ratio of characteristic phonon frequency to cyclotron frequency is large. The calculations are carried out for GaAs quantum wells where PIRO have been observed experimentally. This includes the cases of 2D electron gas with high density and moderate mobility[14] and with lower density and very high mobility.[17] The calculated magnetoresistance is in agreement with experimental data. As concerns the positions of the magnetoresistance peaks, the agreement is very good in the case of high-mobility systems.[17]

Based on the results obtained, one may conclude that the bulk approximation for description of acoustic phonon modes and of their interaction with 2D electrons works reasonably good in application to magnetotransport in GaAs quantum wells. Another important conclusion is that the velocity s in the empirical Eq. (1) does not, in general, correspond to a certain phonon mode. The reason for this is the complicated structure of the phonon spectrum. There are three anisotropic phonon modes (branches) with different velocities and two mechanisms, deformation-potential and piezoelectric, of electron-phonon interaction. Relative contributions of these modes and of the interaction mechanisms depend on 2D electron density, temperature, and other parameters such as the width of the quantum well and growth direction. This explains why the velocity s determined by fitting the experimental PIRO peak positions is expected to vary in different experiments, especially when such a fit is based upon a few low-order peaks which have the highest amplitudes and, therefore, are best visible experimentally. Indeed, the low-order peaks are typically formed as a superposition of contributions from different modes, and even for each single mode there is a mixture of phonons with different velocities owing to the anisotropy. The anisotropy influences not only the frequency but also the phase and the amplitude of the oscillations.

On the other hand, in the region of high-order magnetophonon resonances the resistance oscillations are described by a fixed set of phonon velocities determined here for the case of [001]-grown quantum wells; see Eqs. (17)–(20). The phases of these oscillations also become definite. Moreover, if the density of 2D electrons is not large, so the piezoelectric-potential interaction is significant, the main contribution to magnetoresistance oscillations in [001]-grown wells is characterized by a single velocity $s=s_{T0}\equiv\sqrt{c_{44}/\rho}$ corresponding to a TA mode propagating in the quantum well plane and polarized perpendicular to this plane. This is the case of experiment Ref. 17, where many magnetoresistance oscillations have been observed owing to a very high-electron mobility. For the wells whose growth axes are different from [001] the characteristic phonon velocities have to be different. These cases are not studied here in detail because PIRO have not yet been observed in such wells. Nevertheless, based on the consideration presented in Sec. III, the following general method for determination of characteristic phonon velocities in the wells of arbitrary growth axis is proposed. Take the surfaces of equal frequency ω defined for each mode in the $\mathbf{q}$-space by the equation $s_{\varphi\chi}^{(\lambda)}q=\omega$. Find the points (numbered by the index i) where these surfaces touch the surface of the cylinder of radius $2p_F/\hbar$ and axis along the growth direction (this cylindrical surface is given by the equation $q\sin\chi=2p_F/\hbar$). The set of frequencies $\omega=\omega_{\lambda i}$ (or, equivalently, velocities $s_{\lambda i}=\omega_{\lambda i}/q$) corresponding to these points will give a set of oscillating harmonics with arguments $2\pi k\omega_{\lambda i}/\omega_c$ in the magnetoresistance. An equivalent procedure is the search for extrema of the function $s_{\varphi\chi}^{(\lambda)}/\sin\chi$, as described in Sec. III. To find which frequencies out of $\omega_{\lambda i}$ give the main contribution and to determine the phases and amplitudes of the oscillations, a detailed analysis is necessary. In the case of [001]-grown wells a single TA mode gives the main contribution [Eq. (18)] because the surface of equal frequency for this particular mode touches the cylinder not just in a finite number of points, but along the whole circumference of the cylinder at $\chi=\pi/2$.

To study the influence of different phonon modes on the magnetoresistance oscillations, it is desirable to carry out experiments in high-mobility 2D systems with densities varied in the range $4-10\times10^{11}$ cm^{-2}. If it is possible to reach high mobilities for the structures with growth axes different from [001], measurements of the oscillating magnetoresistance in such systems would be also important for investigation of the phonon anisotropy effects discussed above. The author hopes that the present theoretical work may stimulate such experiments.

The consideration given in this paper assumes the linear response regime, when both electron and phonon systems are close to equilibrium. One may expect a more interesting and rich behavior of the phonon-induced resistance oscillations under nonlinear transport regime when the electric current through the sample increases. Studies in this direction are already undertaken.[15,16] In addition to the work already done, more efforts, both experimental and theoretical, are necessary for better understanding of the mechanisms of phonon-induced oscillations and their interplay with the other microscopic mechanisms responsible for the magnetoresistance of 2D electrons at large filling factors.

[1] M. A. Zudov, R. R. Du, J. A. Simmons, and J. L. Reno, Phys. Rev. B **64**, 201311(R) (2001).
[2] R. G. Mani, J. H. Smet, K. von Klitzing, V. Narayanamurti, W. B. Johnson, and V. Umansky, Nature (London) **420**, 646 (2002).
[3] M. A. Zudov, R. R. Du, L. N. Pfeiffer, and K. W. West, Phys. Rev. Lett. **90**, 046807 (2003).
[4] W. Zhang, H. S. Chiang, M. A. Zudov, L. N. Pfeiffer, and K. W. West, Phys. Rev. B **75**, 041304(R) (2007).
[5] J.-q. Zhang, S. Vitkalov, A. A. Bykov, A. K. Kalagin, and A. K. Bakarov, Phys. Rev. B **75**, 081305(R) (2007).
[6] C. L. Yang, J. Zhang, R. R. Du, J. A. Simmons, and J. L. Reno, Phys. Rev. Lett. **89**, 076801 (2002).
[7] A. A. Bykov, J. Q. Zhang, S. Vitkalov, A. K. Kalagin, and A. K. Bakarov, Phys. Rev. B **72**, 245307 (2005).
[8] N. C. Mamani, G. M. Gusev, T. E. Lamas, A. K. Bakarov, and O. E. Raichev, Phys. Rev. B **77**, 205327 (2008).
[9] A. A. Bykov, D. P. Islamov, A. V. Goran, and A. I. Toropov, JETP Lett. **87**, 477 (2008).
[10] M. A. Zudov, I. V. Ponomarev, A. L. Efros, R. R. Du, J. A. Simmons, and J. L. Reno, Phys. Rev. Lett. **86**, 3614 (2001).
[11] J. Zhang, S. K. Lyo, R. R. Du, J. A. Simmons, and J. L. Reno, Phys. Rev. Lett. **92**, 156802 (2004).
[12] V. L. Gurevich and Y. Firsov, Sov. Phys. JETP **13**, 137 (1961).
[13] See, for example, D. C. Tsui, T. Englert, A. Y. Cho, and A. C. Gossard, Phys. Rev. Lett. **44**, 341 (1980).
[14] A. A. Bykov, A. K. Kalagin, and A. K. Bakarov, JETP Lett. **81**, 523 (2005).
[15] W. Zhang, M. A. Zudov, L. N. Pfeiffer, and K. W. West, Phys. Rev. Lett. **100**, 036805 (2008).
[16] X. L. Lei, Phys. Rev. B **77**, 205309 (2008).
[17] A. T. Hatke, M. A. Zudov, L. N. Pfeiffer, and K. W. West, Phys. Rev. Lett. **102**, 086808 (2009).
[18] M. G. Vavilov and I. L. Aleiner, Phys. Rev. B **69**, 035303 (2004).
[19] I. A. Dmitriev, M. G. Vavilov, I. L. Aleiner, A. D. Mirlin, and D. G. Polyakov, Phys. Rev. B **71**, 115316 (2005).
[20] www.ioffe.ru/SVA/NSM/Semicond/GaAs/mechanic.html.
[21] Some data suggest that the value of the piezoelectric constant h_{14} in GaAs is higher than 1.2 V/nm usually used in the literature: V. W. L. Chin, Solid-State Electron. **37**, 1345 (1994).
[22] Phonon-assisted scattering also leads to temperature dependence of quantum lifetime. However, the corresponding additional contribution to the inverse quantum lifetime is of the order of background phonon-assisted transport rate $\nu_{ph}^{(0)}$ and is much smaller than $1/\tau_q$ caused by electron-impurity scattering.